Int. J. Solids Structures Vol. 25, No. 7, pp. 751–768, 1989
Printed in Great Britain.

0020-7683/89 $3.00 + .00

ELASTIC BUCKLING AND POSTBUCKLING OF ECCENTRICALLY STIFFENED PLATES

EIVIND STEEN
Det norske Veritas, VMS 261, Veritasvn 1, 1322 Høvik, Norway

(*Received* 26 *May* 1988; *in revised form* 24 *October* 1988)

Abstract—The elastic buckling and postbuckling behaviour of eccentrically stiffened plates are evaluated analytically. The effects of lateral boundary conditions and of stiffener eccentricity relative to the plate plane are emphasized. Attention is confined to global buckling; local plate and local stiffener buckling effects are neglected. A simplified direct energy approach is used together with Marguerre's plate theory. Critical buckling loads are found which are generally higher than those obtained with a simple Euler column model. A simple closed-form solution is found for the postbuckling curve which for small imperfection levels coincides with the classical Koiter solution. The buckling behaviour is found to be asymmetric with loads generally in excess of the critical load in the advanced postbuckling region.

1. INTRODUCTION

Buckling of stiffened plates is a subject of continuous interest due to their extensive application in steel structures.

The published results on buckling of stiffened plates follow three separate routes:

(i) the orthotropic plate approach;
(ii) the column approach;
(iii) the discretely stiffened plate approach.

An example of the first category is given in Mansour (1971). The stiffeners are smeared out over the plate and the final nonlinear equilibrium and compatability conditions are solved numerically. Examples of linear buckling analyses of stiffened plates by the orthotropic method may be found in Timoshenko and Gere (1961) and Troitsky (1976).

The column approach for stiffened plate analysis is widely used in design codes due to its simplicity, e.g. Det norske Veritas (1987). It has also been used extensively for studying interaction phenomena between local and global buckling in stiffened panels (Koiter and Pignataro, 1974; van der Neut, 1974; Tulk and Walker, 1976).

Several attempts have also been made to consider the discrete effects of the stiffeners on the buckling behaviour. Notable among these are Tvergaard (1973), Ueda and Yao (1983), Jetteur (1983). The present paper is a similar attempt along this "third route" to analyse the stiffened plate considering the stiffeners as discrete elements attached to the plate along distinct lines. Only global buckling involving lateral deflections of the stiffeners is considered; i.e. possible mode interactions between local plate/stiffener and global panel buckling are neglected, see Fig. 3.

By means of a direct energy method, with a simple assumption for the out-of-plane deflection form, a compact and very simple closed-form solution is obtained.

The main interest is on buckling of rectangular plates having width-to-length ratio in the range of

$$d/a = [0.5, 2].$$

See Fig. 1(a) and (b) for geometrical properties of the stiffened panel.

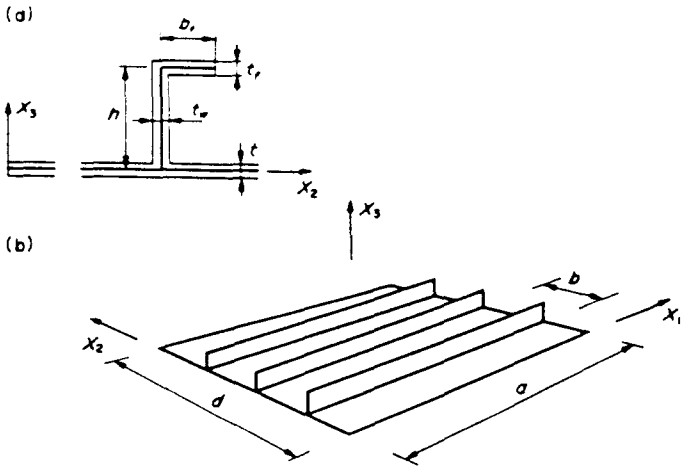

Fig. 1. (a) Stiffener geometry idealization; (b) stiffened panel geometry.

2. THEORETICAL MODEL

Fundamentals

The stiffened plate model is particularly intended to simulate the behaviour of panels used in steel ships and offshore structures. Stiffened panels in such structures are supported laterally by a stiff system of cross-frames and longitudinal girders. The panels normally span several bays and the stiffeners run continuously through cut-outs in the webs. A consequence of this lay-out is that the lateral support is provided at the edges of the plate itself on all boundaries. This will be shown to be a significant difference from the normal assumption of lateral support of the neutral surface of a stiffener/plate combination (see Fig. 2).

Basic assumptions

The stiffened panel considered is shown in Fig. 1(a); the stiffeners and their attachment to the plate are shown in Fig. 1(b). The height of the stiffeners is assumed to be an order of magnitude larger than the plate and flange thicknesses, and the web's middle plane is attached to the plate's middle plane.

The plate theory used is due to Marguerre (1937). Thus the membrane strains of the middle plate plane are taken to be

$$\begin{aligned}\varepsilon_1 &= u_{,1} + \tfrac{1}{2}w_{,1}^2 + w_{0,1}w_{,1}\\ \varepsilon_2 &= v_{,2} + \tfrac{1}{2}w_{,2}^2 + w_{0,2}w_{,2}\\ \gamma_{12} &= u_{,2} + v_{,1} + w_{,1}w_{,2} + w_{0,1}w_{,2} + w_{0,2}w_{,1}\end{aligned} \tag{1}$$

where u, v and w are the additional displacements of the plate's middle surface in the x_1,

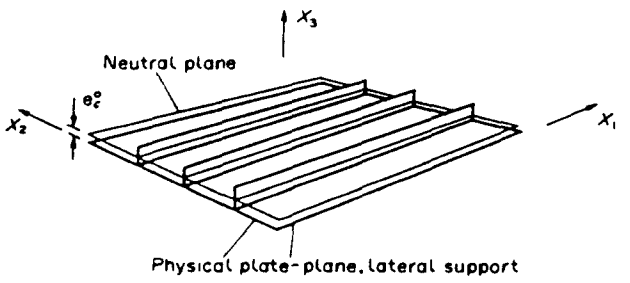

Fig. 2. Lateral support conditions.

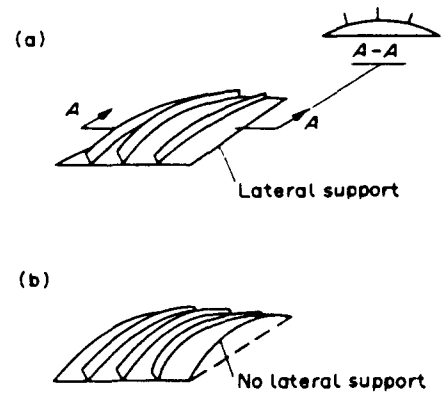

Fig. 3. Stiffened plate models, global buckling mode. (a) Present stiffened plate model; (b) column model (Perry Robertson).

x_2 and x_3 directions respectively, and w_0 is the stress-free initial imperfection. The bending strains are given by

$$\kappa_1 = -w_{,11}$$
$$\kappa_2 = -w_{,22}$$
$$\kappa_{12} = -w_{,12}. \tag{2}$$

The Love–Kirchhoff assumption is taken to be valid also for the stiffeners. This leads to a simple relation for the strain at a given point

$$\bar{\varepsilon}_1 = \varepsilon_1 - x_3 w_{,11}$$
$$\bar{\varepsilon}_2 = \varepsilon_2 - x_3 w_{,22}$$
$$\bar{\gamma}_{12} = \gamma_{12} - 2x_3 w_{,12}. \tag{3}$$

It is emphasized that the relation for $\bar{\varepsilon}_1$ in eqn (3) is only an approximation for the strain distribution in a stiffener. However, it is thought to be sufficiently accurate for the present problem in which local plate/stiffener buckling is neglected.

Strain energy

The strain energy of a three-dimensional, linear-elastic, anisotropic medium is generally expressed as (Brush and Almroth, 1975)

$$U = \frac{1}{2}\int \bar{\sigma}_{ij}\bar{\varepsilon}_{ij}\,\mathrm{d}V \tag{4}$$

in which $\bar{\sigma}_{ij}$ and $\bar{\varepsilon}_{ij}$ represent the stress and strain tensor components respectively at a given point. Applying the normal thin-plate assumptions, namely Hooke's law for plane stress in the plate and uniaxial stress distribution for the stiffeners, this expression can be rewritten as

$$U = \frac{E}{2(1-\nu^2)}\int_{V_p}\left(\bar{\varepsilon}_1^2 + \bar{\varepsilon}_2^2 + 2\nu\bar{\varepsilon}_1\bar{\varepsilon}_2 + \frac{1-\nu}{2}\bar{\gamma}_{12}^2\right)\mathrm{d}V + \frac{E}{2}\int_{V_s}\bar{\varepsilon}_1^2\,\mathrm{d}V. \tag{5}$$

Integration is taken over the initial plate volume V_p and stiffener volume V_s. Substituting eqn (3) into the expression for the strain energy eqn (5) gives for U,

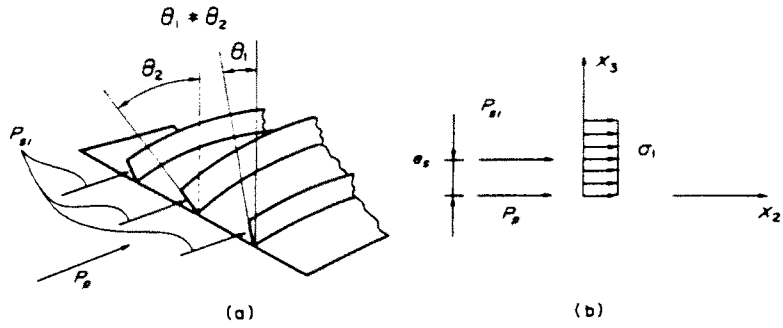

Fig. 4. External force system.

$$U = \frac{E}{2(1-\nu^2)}\int_{V_p}(w_{,11}^2 + w_{,22}^2 + 2\nu w_{,11}w_{,22} + 2(1-\nu)w_{,12}^2)x_3^2\,\mathrm{d}V + \frac{E}{2(1-\nu^2)}\int_{V_p}\left(\varepsilon_1^2 + \varepsilon_2^2 + 2\nu\varepsilon_1\varepsilon_2 + \frac{1-\nu}{2}\gamma_{12}^2\right)\mathrm{d}V + \frac{E}{2}\int_{V_s} w_{,11}^2 x_3^2\,\mathrm{d}V - E\int_{V_s} w_{,11}\varepsilon_1 x_3\,\mathrm{d}V + \frac{E}{2}\int_{V_s}\varepsilon_1^2\,\mathrm{d}V. \quad (6)$$

An examination of this expression for the strain energy reveals a *non-zero coupling term* between out-of-plane deflection w and in-plane displacement u. It originates from the basic assumption of lateral support along the plate edges and demonstrates that the conventional *first order approximation* in plate theory of decoupled bending and membrane strain energies does not generally apply for stiffened plate and shell structures.

Since only global buckling is considered herein, some further simplifications were introduced with respect to the strain energy calculation of *the stiffeners*. Physically this simplification amounts to lumping all the stiffener material onto the x_1-axes (in particular the flange was considered as a material point). In this way their sideways bending and torsional stiffnesses were conservatively neglected.

External loading

The stiffened panel is subjected to a uniaxial loading in the stiffener direction. In order to facilitate a type of external loading which is compatible with the boundary conditions, the external loading is split into two separate independent systems:

(i) the plate load P_p;
(ii) the stiffener forces $P_{st,i} = 1, 2, \ldots, N$

where N is the number of stiffeners (see Fig. 4). This splitting of the external load is crucial in the present analysis as it provides a consistent calculation of the external energy as explained below.

Compatability and constraint conditions

Marguerre's plate theory gives the following compatability condition between out-of-plane and in-plane deflections for plates.

$$\nabla^4 F = E[(w_0+w)_{,12}^2 + w_{0,11}w_{0,22} - w_{0,12}^2 - (w_0+w)_{,11}(w_0+w)_{,22}]. \quad (7)$$

Here F is the Airy stress function defined as

$$\sigma_1 = F_{,22}$$
$$\sigma_2 = F_{,11}$$

$$\sigma_{12} = -F_{,12}. \tag{8}$$

σ_1, σ_2, and σ_{12} are the membrane stresses in the plate plane, $x_3 = 0$.

Compatibility between plate and stiffeners is ensured by prescribing the same strain distribution in the plate and stiffeners along their junction lines. This last *constraint* makes it possible to express the plate force in terms of the stiffener forces. A consequence of this is that the redistribution of stiffener forces transversely is coped with.

External energy

The splitting of the external loading into two separate sets of loads makes it possible to consider the geometrical fact that the different stiffener forces produce different amounts of external energy. This is due to the different angle rotation at the support of the stiffeners (see Fig. 4(a)), i.e.

$$\theta_i = \theta_i(x_{2i}), \quad i = 1, \ldots, N \ (i \text{ not summed}). \tag{9}$$

Simply supported boundary conditions ensure a uniform stress condition along the height of the stiffeners at supports. Thus all stiffener forces act during deformation at the same distance e_s from the plate plane (Fig. 4(b)). The expression for the external energy reads

$$T = -2\sum_{s=1}^{N} P_s u_s - P_p u_p \quad (s, p \text{ not summed}). \tag{10}$$

Here u_s is the in-plane displacement of the different stiffeners evaluated at *the position* $x_3 = e_s$ (at support $x_1 = 0$, $x_1 = a$). u_p is the in-plane displacement of the plate edge which is constrained to remain straight during deformation. The Love Kirchhoff assumption leads to the final expression for the external energy

$$T = 2\sum_{s=1}^{N} P_s e_s w_{,1} - P u_p \quad (s \text{ not summed}). \tag{11}$$

$w_{,1}$ is evaluated at discrete stiffener positions x_{2i} and P is the total force acting in the panel, i.e.

$$P = P_p + \sum_{s=1}^{N} P_s. \tag{12}$$

Deflection form/boundary conditions

The results presented are based on a very simple assumption for the lateral deflection forms. Additional out-of-plane deflection w is taken as

$$w = w_1 \sin\frac{\pi}{a}x_1 \sin\frac{\pi}{d}x_2. \tag{13}$$

The geometrical imperfection is taken in the same form as

$$w_0 = \delta \sin\frac{\pi}{a}x_1 \sin\frac{\pi}{d}x_2. \tag{14}$$

This corresponds to the first term in a general Fourier series for deflection description and satisfies the condition for simply supported edges. Then $w_{,11} = 0$ along the edges leads to a uniform strain distribution over the stiffener height at support, as previously stated. The mechanical boundary conditions ensure equilibrium between external and internal forces in the following form:

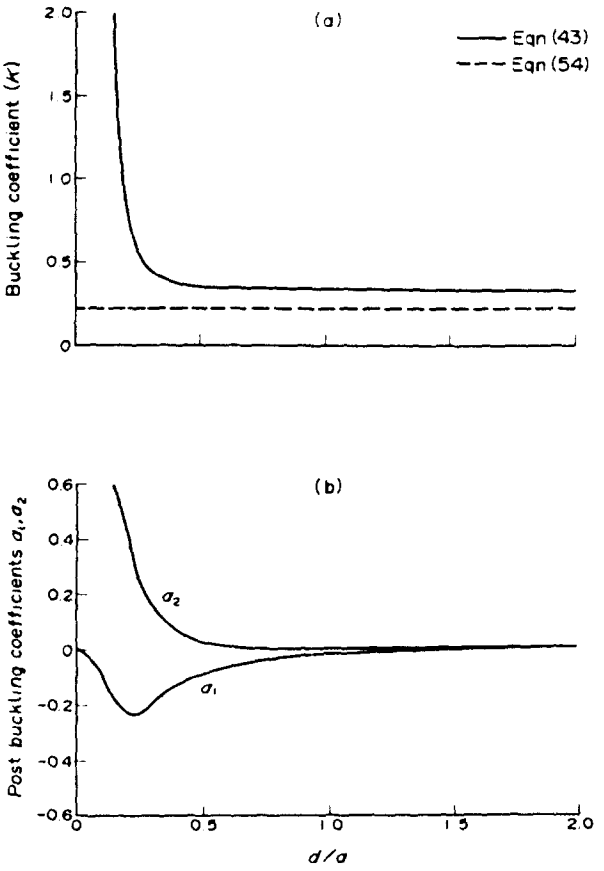

Fig. 5. (a) Buckling coefficient; (b) postbuckling coefficient, for example $N = 6$, $a_1 = 0.3$, $a_t = 0$, $h/t = 15$.

$$P_p + \sum_{i=1}^{N} P_{si} = -\int_{A_p} \sigma_1 \, dA - \sum_{i=1}^{N} \int_{A_s} \sigma_1 \, dA \tag{15}$$

in which we prescribe (Fig. 5(b))

$$P_p = -\int_{A_p} \sigma_1 \, dA$$

$$P_{si} = -\int_{A_s} \sigma_1 \, dA, \quad \text{at stiffener positions } x_{2i}. \tag{16}$$

Integration is taken over the plate area A_p and stiffener cross-sectional areas A_s.

Moment equilibrium about $x_3 = 0$ at support is ensured if

$$P_{si} e_s = -\int_{A_s} \sigma_1 x_3 \, dA, \quad \text{at stiffener positions } x_{2i}. \tag{17}$$

This gives for e_s

$$e_s = (\tfrac{1}{2}h^2 t_s + b_f t_f h)/A_s. \tag{18}$$

For the internal stress distribution positive stresses are in tensile and for the external loading positive forces are in compression; see Fig. 4(b). These prescribed mechanical boundary

conditions are essential for the results as found and they are thought to represent a realistic set for practical application for a *continuously stiffened panel.*

3. ANALYSIS

Substituting the deflection forms of eqns (13) and (14) into Marguerre's compatibility equation for the plate, eqn (7), gives the following solution for Airy's stress function.

$$F = -\tfrac{1}{2}x_1^2\sigma_{10} + \frac{Et^2}{32}(2\delta w_1 + w_1^2)\left[\left(\frac{d}{a}\right)^2 \cos\frac{2\pi}{d}x_2 + \left(\frac{a}{d}\right)^2 \cos\frac{2\pi}{a}x_1\right]. \tag{19}$$

σ_{10} is the average stress in the plate. Equation (19) gives, by applying the definitions of eqn (8) the following form of the membrane stress distribution in the plate

$$\begin{aligned}
\sigma_1 &= -\sigma_{10} - \frac{\pi^2}{8}E\left(\frac{t}{a}\right)^2(2\bar{\xi}\xi + \xi^2)\cos\frac{2\pi}{d}x_2 \\
\sigma_2 &= -\frac{\pi^2}{8}E\left(\frac{t}{d}\right)^2(2\bar{\xi}\xi + \xi^2)\cos\frac{2\pi}{a}x_1 \\
\sigma_{12} &= 0.
\end{aligned} \tag{20}$$

Here ξ and $\bar{\xi}$ are the non-dimensional deflection amplitudes w_1 and δ, respectively:

$$\begin{aligned}
\xi &= \frac{w_1}{t} \\
\bar{\xi} &= \frac{\delta}{t}.
\end{aligned} \tag{21}$$

There are consequently no shear stresses in the plate; the stresses vary only normal to the direction in which they act. Applying Hooke's law for plane stress gives the corresponding membrane strain distribution

$$\begin{aligned}
\varepsilon_1 &= -\frac{1}{E}\sigma_{10} - \frac{\pi^2}{8}(2\bar{\xi}\xi + \xi^2)\left[\left(\frac{t}{a}\right)^2 \cos\frac{2\pi}{d}x_2 - \nu\left(\frac{t}{d}\right)^2 \cos\frac{2\pi}{a}x_1\right] \\
\varepsilon_2 &= \frac{\nu}{E}\sigma_{10} - \frac{\pi^2}{8}(2\bar{\xi}\xi + \xi^2)\left[\left(\frac{t}{d}\right)^2 \cos\frac{2\pi}{a}x_1 - \nu\left(\frac{t}{a}\right)^2 \cos\frac{2\pi}{d}x_2\right] \\
\gamma_{12} &= 0.
\end{aligned} \tag{22}$$

There are no shear strains in the plate and the normal strain distributions vary both longitudinally and transversely.

From Marguerre's kinematic relation, eqn (1), eqns (13) (14) and (22), the relative end-shortening of the panel is

$$\begin{aligned}
u(x_1 = a) - u(x_1 = 0) &= \int_0^a u_{,1}\,\mathrm{d}x_1 = -\frac{1}{E}\sigma_{10}a - \frac{\pi^2}{8}(2\bar{\xi}\xi + \xi^2)\left(\frac{t}{a}\right)^2 a \\
v(x_2 = d) - v(x_2 = 0) &= \int_0^d v_{,2}\,\mathrm{d}x_2 = \frac{\nu}{E}\sigma_{10}d - \frac{\pi^2}{8}(2\bar{\xi}\xi + \xi^2)\left(\frac{t}{d}\right)^2 d.
\end{aligned} \tag{23}$$

It is noted that u and v evaluated at the edges are constants.

This illustrates that the conditions of straight edges remaining straight during deformation is satisfied and is a direct consequence of the prescribed compatability conditions, eqn (7), and out-of-plane deflection form, eqn (13).

Defining the relative scaled shortening of two opposite plate edges Δ_1 and Δ_2 as

$$\Delta_1 = \frac{u(x_1 = 0)}{a}; \quad u(x_1 = a) = 0$$

$$\Delta_2 = \frac{v(x_2 = 0)}{d}; \quad v(x_2 = d) = 0 \tag{24}$$

gives the load-shortening–deflection relations

$$\Delta_1 = \frac{1}{E}\sigma_{10} + \frac{\pi^2}{8}\left(\frac{t}{a}\right)^2(2\bar{\xi}\xi + \xi^2)$$

$$\Delta_2 = -\frac{\nu}{E}\sigma_{10} + \frac{\pi^2}{8}\left(\frac{t}{d}\right)^2(2\bar{\xi}\xi + \xi^2). \tag{25}$$

The interesting equation is the first in eqns (25) and this is alternatively written

$$\sigma_{10} = E\Delta_1 - \frac{\pi^2}{8}E\left(\frac{t}{a}\right)^2(2\bar{\xi}\xi + \xi^2). \tag{26}$$

The strain distribution along a junction line of stiffener and plate in the position x_{2i} is, directly from eqn (22)

$$\varepsilon_{1i} = -\frac{1}{E}\sigma_{10} - \frac{\pi^2}{8}(2\bar{\xi}\xi + \xi^2)\left[\left(\frac{t}{a}\right)^2 \cos\frac{2\pi}{d}x_{2i} - \nu\left(\frac{t}{d}\right)^2 \cos\frac{2\pi}{a}x_1\right]. \tag{27}$$

Then the expression for a stiffener force is

$$P_{si} = -\int_{A_s} E\varepsilon_{1i}(x_1 = 0)\,\mathrm{d}A$$

$$P_{si} = A_s\sigma_{10} + \frac{\pi^2}{8}(2\bar{\xi}\xi + \xi^2)\left[\left(\frac{t}{a}\right)^2 \cos\frac{2\pi}{d}x_{2i} - \nu\left(\frac{t}{d}\right)^2\right]EA_s. \tag{28}$$

The total force carried by the stiffeners is

$$P_s = \sum_{i=1}^{N} P_{si}, \tag{29}$$

i.e.

$$P_s = NA_s\sigma_{10} - \frac{\pi^2}{8}(2\bar{\xi}\xi + \xi^2)\left[N\nu\left(\frac{t}{d}\right)^2 + \left(\frac{t}{a}\right)^2\right]EA_s.$$

In this way the average stress in the stiffened panel σ_{p1} is defined as

$$\sigma_{p1} = \frac{P}{NA_s + \mathrm{d}t} \tag{30}$$

where P is the total force.

σ_{p1} may be expressed as a function of the average stress in the plate σ_{10} defined as

$$\sigma_{10} = \frac{P_p}{td}. \tag{31}$$

The relation between σ_{p1} and σ_{10} is found as

$$\sigma_{p1} = \sigma_{10} - \frac{\pi^2}{8} E \frac{a_s}{N} (2\bar{\xi}\xi + \xi^2) \left[Nv \left(\frac{t}{d}\right)^2 + \left(\frac{t}{a}\right)^2 \right] \tag{32}$$

in which the area coefficient a_s is introduced (see Appendix for definition).

For no stiffeners ($a_s = 0$) $\sigma_{p1} = \sigma_{10}$.

This gives the final load-shortening–deflection-relation as

$$\sigma_{p1} = E\Lambda_1 - \frac{\pi^2}{8} E(2\bar{\xi}\xi + \xi^2) \left[a_s v \left(\frac{t}{d}\right)^2 + \left(1 + \frac{a_s}{N}\right) \left(\frac{t}{a}\right)^2 \right]. \tag{33}$$

By satisfying the compatability conditions for the plate it is possible to eliminate the in-plane displacements u and v. This simplifies the final result considerably and the expression for the potential energy is expressed as a function *of the single out-of-plane coordinate* ξ.

Potential energy

$$V = U + T. \tag{34}$$

After substituting the stress and strain distributions the expression for V can be written in the following compact form (per unit plate volume)

$$V = k_1 \sigma_{p1} (2\bar{\xi}\xi + \xi^2) + b_{11}\xi^2 + b_{111}\xi(2\bar{\xi}\xi + \xi^2) + b_{1111}(2\bar{\xi}\xi + \xi^2)^2.$$

The coefficients k_1, b_{11}, b_{111} and b_{1111} are given in the Appendix.

4. RESULTS

For convenience the subscripts $_p$ and $_1$ for load in stiffener direction are omitted in the presentation of the results.

Applying the principle of stationary potential energy gives the following closed-form solution for the equilibrium path:

$$\frac{\sigma}{\sigma_c} = \frac{\xi}{\bar{\xi} + \xi} [1 + a_1(\xi + \tfrac{1}{2}\bar{\xi}) + a_2(\xi^2 + 3\bar{\xi}\xi + 2\bar{\xi}^2)] \tag{35}$$

where a_1 and a_2 are the postbuckling coefficients given by

$$a_1 = \frac{3}{2}\frac{b_{111}}{b_{11}}$$

$$a_2 = \frac{b_{1111}}{b_{11}} \tag{36}$$

and σ_c is the critical stress.

The postbuckling coefficients have the simple form

$$a_1 = -\frac{48}{\pi}(1-\nu^2)\nu\frac{h}{t}\frac{\phi_2\phi_3}{\psi}$$

$$a_2 = \frac{3}{4}\frac{(1-\nu^2)}{1-a_s}\left(\frac{d}{a}\right)^2\frac{1}{\psi}\left[(2a_s^2\nu^2+1-a_s+a_s\nu^2)\left(\frac{a}{d}\right)^4+\frac{N-a_s}{N}-2\left(\frac{a_s}{N}\right)^2\right]. \tag{37}$$

Expressions for the geometrical coefficients ϕ_1, ϕ_2, ϕ_3, a_s and ψ are given in the Appendix.

Equation (35) resembles the Koiter solution for single mode buckling if the *second order effects* from geometrical imperfections are neglected. The Koiter solution reads (Dym, 1974):

$$\frac{\sigma}{\sigma_c} = \frac{\xi}{\xi+\xi}(1+a_1\xi+a_2\xi^2). \tag{38}$$

Thus the present solution indicates *more optimistic results for imperfect panels than the asymptotic Koiter solution.*

Critical load

The critical buckling stress is found as

$$\sigma_c = C\frac{\pi^2 E}{12(1-\nu^2)}\left(\frac{t}{d}\right)^2 \tag{39}$$

where

$$C = \frac{N(1-a_s)}{N+a_s}\psi \tag{40}$$

and

$$\psi = \left(\frac{a}{d}+\frac{d}{a}\right)^2+12(1-\nu^2)(N+1)\left(\frac{d}{a}\right)^2\left(\frac{h}{t}\right)^2\phi_1. \tag{41}$$

ϕ_1 is given in the Appendix. In eqn (39) the reference will be $C = 4$ corresponding to an unstiffened square plate ($\phi_1 = 0$).

An alternative expression for the critical stress of eqn (39) is

$$\sigma_c = K\frac{\pi^2}{3}E\left(\frac{h}{a}\right)^2 \tag{42}$$

where

$$K = \frac{1}{4(1-\nu^2)} \frac{N(1-a_s)}{N+a_s}\left[\left(\frac{t}{h}\right)^2\left(1+\left(\frac{a}{d}\right)^2\right)^2 + 12(1-\nu^2)(N+1)\phi_1\right]. \tag{43}$$

A necessary condition for eqns (39) and (42) to be valid is

$$1+12(1-\nu^2)(N+1)\left(\frac{h}{t}\right)\phi_1 > \frac{1}{4}\left(\frac{a}{d}\right)^4 \tag{44}$$

corresponding to a single wave in the x_1-direction.

The buckling coefficient K is shown graphically in Fig. 5(a) for the case of

$$\begin{aligned} N &= 6 \\ a_s &= 0.3 \\ a_t &= 0.0 \\ \frac{h}{t} &= 15. \end{aligned} \tag{45}$$

A closer examination of eqn (43) shows that it consists of two terms. Their origins are from the bending stiffness of the plate and stiffeners, respectively. It is important to note that the contribution from the stiffeners results from the bending stiffness of each stiffener about the plate plane and not about their own or combined section's neutral axis. This is due to the fundamental lateral support conditions implemented in the plate plane. For dominating stiffener contribution K simplifies to

$$K = \frac{N}{N+a_s}\left[\frac{N+1}{N}a_s + 2a_t\right] \tag{46}$$

which further for $N \gg 1$ (wide panels) approximates to (area coefficients a_s, a_t given in the Appendix)

$$K = a_s + 2a_t. \tag{47}$$

For comparison is given the classical column (Euler) formula (Fig. 4(b))

$$\sigma_E = \pi^2 E\left(\frac{i}{a}\right)^2 \tag{48}$$

where i is the radius of gyration of the stiffener/plate section. If the stress variations over the plate and flange thickness are neglected consistently with the present model, eqn (48) is transformed to the same format as eqn (42) leading to

$$\sigma_E = K\frac{\pi^2}{3}E\left(\frac{h}{a}\right)^2 \tag{49}$$

where

$$K = g_1 - g_2^2 \tag{50}$$

and

$$g_1 = a_s + 2a_f$$
$$g_2 = \tfrac{1}{4}(a_s + a_f). \tag{51}$$

Note that these formulas are valid for a panel with an equal number of stiffeners and plate elements [model used in Det norske Veritas (1987)].

For wide panels with $N \gg 1$, expressions for K from eqns (47) and (50) are directly comparable. (For $N \gg 1$, wide panels, there is no distinction between a_s, a_f and a'_s, a'_f, respectively.) It is seen for small stiffening ratios (a_s, a_f are small) that the column formula and the present coincide, while for larger area ratios the difference in the buckling coefficient K will be significant. This is consistent with the fact that the difference in calculating moment of inertia about the cross-section's neutral axis and the plate plane respectively increases as the stiffening increases.

A stiffened panel in the present context consists of one plate element more than stiffeners, so in order to compare eqn (50) with the present formula (eqn (43)) an area correction is necessary.

Then in Fig. 5(a) is also shown σ_E^* where

$$\sigma_E^* = \frac{N + a_s}{N + 1}\sigma_E, \tag{52}$$

i.e.

$$\sigma_E^* = K\frac{\pi^2}{3}E\left(\frac{h}{a}\right)^2 \tag{53}$$

where

$$K = \frac{N + a_s}{N + 1}(g_1 - g_2^2). \tag{54}$$

The horizontal asymptotes in Fig. 5(a) correspond to column buckling which dominates for wide panels $d/a > 1$. For $d/a < 1$ the "plate effect" becomes apparent, especially so for light stiffening.

Postbuckling behaviour

From the form of the equilibrium path given by eqn (35) it is clear that the buckling behaviour is asymmetric. The postbuckling coefficients a_1 and a_2 describes the slope and curvature respectively of the load–deflection curve at buckling. a_1 takes always negative values indicating an initially unstable behaviour when the panel buckles in the stiffener direction. The physical explanation for this is that stiffeners buckling in the stiffener direction will lengthen in the immediate vicinity after the bifurcation load, relative to the unbuckled stiffener at σ_s. Subjected to compression this is a condition the stiffeners seek to avoid. Then just after buckling the stiffener will *exhaust* this elongation preferring an unstretched, or rather, compressed state. This leads to the *initial unstable behaviour before higher order membrane effects in the plate stabilize the response*. For panels buckling in the plate direction the stiffeners are at buckling shortened, which is a state that will prevail during further compression. Thus the behaviour in this direction is stable.

For some special geometries (in which only one stiffener is present) the coefficient a_2 takes negative values. Though for practical geometries its numerical value will be small at the same time as a_1 is small. This indicates then an almost neutral behaviour.

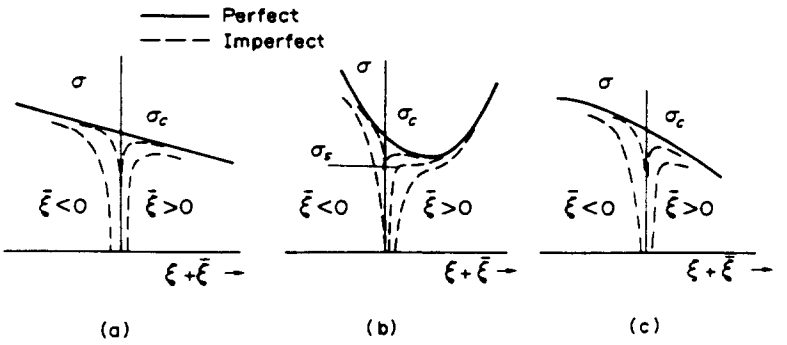

Fig. 6. Non-linear response of perfect and imperfect stiffened plates. (a) $a_1 < 0$, $a_2 = 0$; (b) $a_1 < 0$, $a_2 > 0$; (c) $a_1 < 0$, $a_2 < 0$.

The possible equilibrium curves are summarized in Fig. 6. Case (b) corresponds to the most practical situation for stiffened panels and illustrates the panels' ability to carry loads in excess of σ_c for large deflections.

It is noted that the present solution gives for an unstiffened ($\phi_1 = \phi_2 = \phi_3 = 0$) square plate symmetric behaviour with postbuckling coefficients

$$a_1 = 0$$
$$a_2 = \tfrac{1}{8}(1 - \nu^2).$$

This resembles the "classical solution" given for example in Dym (1974).

The postbuckling coefficients a_1 and a_2 (eqns (37)) are shown graphically in Fig. 5(b) for the example given by eqn (45). Related to the results shown for the critical stress in Fig. 5(a) this shows that for $d/a < 1$ the obvious "plate effect" raising the critical stress is accompanied by an initial unstable postbuckling behaviour. For more wide panels $d/a > 1$ the postbuckling will be more neutral indicating the "column contribution" to be an effective limit for the elastic buckling capacity.

Imperfect panels

For panels with geometrical imperfections the equilibrium curves are illustrated in Fig. 6 as dotted lines. When $a_2 > 0$ (which is the most practical case) there exists for small imperfections $\bar{\xi}$ a local limit load σ_s less than σ_c; $\sigma_s < \sigma_c$ as indicated in Fig. 6. An explicit expression for the limit load σ_s is not found since it involves the solution of a third-order equation

$$f_1\xi^3 + f_2\xi^2 + f_3\xi + f_4 = 0. \tag{55}$$

A notable feature of the equilibrium path for imperfect panels exists in this case ($a_2 > 0$). This consists of a continuously rising load–deflection curve for a geometrical imperfection beyond a critical value, i.e. for

$$\bar{\xi} > \bar{\xi}_c \quad (\bar{\xi}_c > 0). \tag{56}$$

The cubic form of eqn (55) makes it impossible to solve for $\bar{\xi}_c$ explicitly.

Edge moments

A further consequence of the assumed lateral boundary conditions is that they lead to edge moments in *the stiffeners*. By using again the column model as a reference it is natural

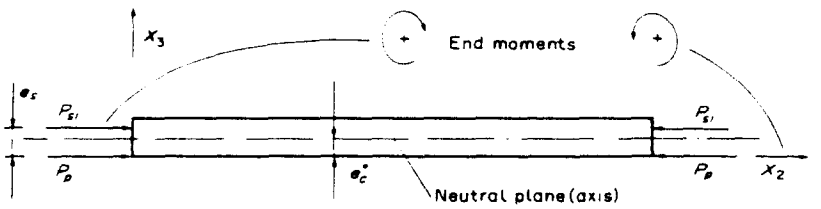

Fig. 7. End-moments reference.

to evaluate the edge moments about the neutral axis of the combined stiffener/plate section located a distance e_c^o from the plate plane (Fig. 7). The moment is

$$M = \sum_{i=1}^{N} P_{si}(e_s - e_c^o) - P_p e_c^o. \tag{57}$$

Substituting for P_{si} and P_p gives

$$\frac{M}{M_c} = c_2(2\bar{\xi}\xi + \xi^2) \tag{58}$$

in which the constant c_2 always takes negative values:

$$c_2 = -\tfrac{1}{2}(1-\nu^2)\frac{N+a_s}{N^2\psi}\left(N\nu + \left(\frac{d}{a}\right)^2\right). \tag{59}$$

The moment M_c is defined as

$$M_c = P_c e_c^o \tag{60}$$

where

$$P_c = \sigma_c(dt + NA_s). \tag{61}$$

Due to the sign convention used (Fig. 7) the moment will always take negative values, that is for perfect panels ($\xi = 0$) the moment works always in the same direction independent of the buckling direction, i.e.

(i) it stiffens the response when the panel deflects in the plate direction;

(ii) it softens the response *when the panel deflects in the* stiffener direction making the situation unstable.

This is consistent with the postbuckling behaviour as explained.

Example

For illustration the postbuckling behaviour of a specific example is evaluated. The stiffened panel analysed has the following geometry

$$N = 6; \quad \frac{h}{t} = 15; \quad a_s = 0.3; \quad \frac{d}{a} = 1; \quad a_t = 0 \text{ (flat bar)}. \tag{62}$$

This gives for the postbuckling coefficients

$$a_1 = -0.0237$$

$$a_2 = 0.0040$$

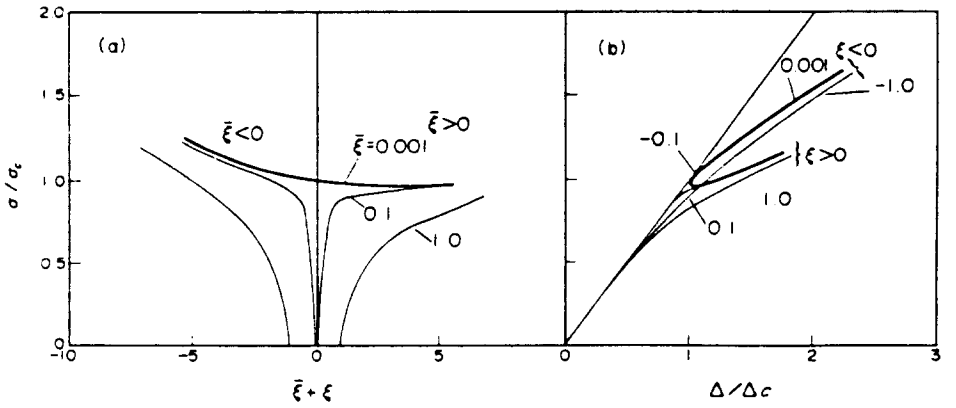

Fig. 8. (a) Load–deflection curve; (b) load end-shortening curve, for example $N = 6$, $h/t = 15$, $a_s = 0.3$, $d/a = 1$, $a_f = 0$ (flat bar).

$$c_2 = -0.0016$$
$$d_2 = 0.0057. \tag{63}$$

The equilibrium solution is

$$\frac{\sigma}{\sigma_c} = \frac{\xi}{\bar{\xi}+\xi}[1 + a_1(\xi + \tfrac{1}{3}\bar{\xi}) + a_2(\xi^2 + 3\bar{\xi}\xi + 2\bar{\xi}^2)] \tag{64}$$

and the load-shortening deflection relation is

$$\frac{\Delta}{\Delta_c} = \frac{\sigma}{\sigma_c} + d_2(2\bar{\xi}\xi + \xi^2). \tag{65}$$

The moment-deflection relationship is

$$\frac{M}{M_c} = c_2(2\bar{\xi}\xi + \xi^2). \tag{66}$$

(Expressions for the postbuckling coefficients a_1, a_2, c_2 and d_2 are given in the Appendix.)

Equations (64) and (65) in which ξ is cross-eliminated are shown in Fig. 8(a) and (b), respectively. Equation (66) is shown in Fig. 9. All relations are shown for three different imperfection levels.

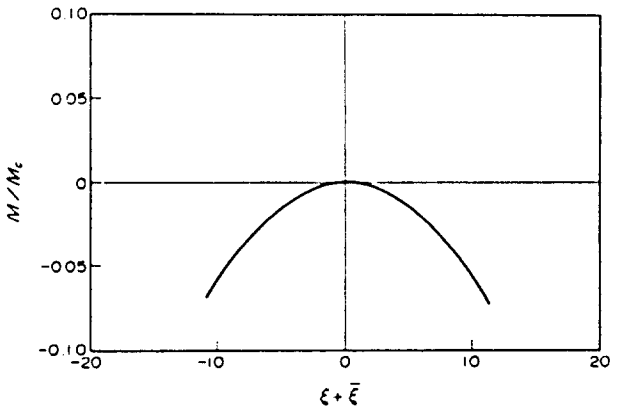

Fig. 9. Moment–deflection, for example $N = 6$, $h/t = 15$, $a_s = 0.3$, $d/a = 1$, $a_f = 0$ (flat bar).

$$\bar{\delta} = 0.001, 0.1, 1.0. \tag{67}$$

Also included is the perfect solution $\bar{\xi} = 0$, though this is not distinguishable from the case for $\bar{\xi} = 0.001$. The asymmetric nature of stiffened plate buckling in the global mode is clearly illustrated by this example.

5. DISCUSSION

The present approach for stiffened plate buckling is based on assumptions of which the most important concern lateral support conditions and the assumed form for the out-of-plane deflection.

Lateral support is provided at the physical plate edges all around the plate and not in the normally assumed neutral plane of the combined plate/stiffener section. These special support conditions are considered to be realistic for panels in which the stiffeners are *continuous* (through cut-outs) over several bays as typically occurs in steel ships and offshore structures. It reflects the physical plate planes' ability to transmit stresses as opposed to the "fictive" neutral plane. The present boundary conditions lead to a coupling between in-plane and out-of-plane displacements which is the indirect cause of the asymmetric behaviour.

The stiffener geometry analysed consisting of flanged or flat bar profiles welded to the plate (Fig. 1(a)) is also typical for steel ships and offshore constructions.

The crude assumption for the form of the out-of-plane deflection leads generally to optimistic results. A more complete series expansion will indicate the magnitude of error introduced. The present approximation improves as the stiffening ratios and d/a ratio reduce.

An important consequence of the present results with respect to asymmetric elastic buckling behaviour found is that it will lead to buckle localizations in structures consisting of several bays of stiffened panels. Signs of such behaviour may be seen in Smith (1975) in which full-scale test results are presented. Including more effects from e.g. local buckling, plasticity, different forms of geometrical imperfections, etc., complicates the picture. The nature of localization of stiffened multispan panels is very similar to the localization in unstiffened plates (Tvergaard and Needleman, 1980).

6. CONCLUSIONS

The elastic buckling and postbuckling of stiffened plates have been evluated analytically. Marguerre's plate theory is applied and the stiffeners are considered as discrete elements.

Only global stiffener buckling has been considered; local plate/stiffener buckling and possible mode interactions being disregarded. Nevertheless, the study of an isolated global buckling deflection has practical interest and reveals new results.

The elastic buckling stress is generally higher than calculated for the *usual Euler column* model in the following sense.

(i) The difference is most notable for panels with a length exceeding its width; then the plate effect is significant.

(ii) The difference is also marked for wide panels and increases rapidly for increasing stiffening ratio. For wide panels ($d/a \gg 1$, $N \gg 1$) a critical buckling stress increase of 8% is noted already for $a_s = 0.1$ ($a_t = 0$). The present wide panel solution is too optimistic.

The postbuckling shows asymmetric behaviour with the initial unstable equilibrium path for panels buckling in the stiffener direction. For larger deflections the behaviour is generally stabilized due to nonlinear membrane effects in the plate leading to possible loads in excess of the critical load. Important conclusions concerning the postbuckling behaviour are as follows.

(i) For panels in which the "plate effect" is notable ($d/a < 1$) the postbuckling behaviour is generally most unstable initially. This is, however, effectively compensated due to

significant nonlinear membrane effects leading to a relatively stiff response after buckling. Stiffness sensitivity due to geometrical imperfections is small.

(ii) For wide panels in which the "column action" dominates the postbuckling behaviour is more neutral. Stiffness reductions due to geometrical imperfections are more marked.

It is emphasized that the present closed-form solution is based on a crude approximation for the deflection surface. This is done in order to highlight the qualitative buckling behaviour of stiffened plates in a simple way capturing the most important parametric dependencies which are otherwise hard to find.

Thus the results are generally optimistic both with respect to the bifurcation load and postbuckling behaviour.

The theoretical foundations are, however, quite general and, with for example a double Fourier expansion of the lateral deflection surface, the present model may be consistently extended to include effects such as shear lag and plate–stiffener buckling interactions.

Acknowledgements—Valuable discussions with Sverre Valsgård, Brian Hayman, Leif Jørgensen and Prof. P. Terndrup Pedersen, DTH, are highly appreciated. Special thanks to Vibeke Wold for her patience with typing this manuscript.

REFERENCES

Brush, D. O. and Almroth, B. O. (1975). *Buckling of Bars, Plates and Shells*. McGraw-Hill, New York.

Det norske Veritas (1987). Buckling strength analysis of mobile offshore units. Class Note No. 30.1, October 1987.

Dym, C. L. (1974). *Stability Theory and its Application to Structural Mechanics*. Noordhoff, Leyden, The Netherlands.

Jetteur, P. (1983). A new design method for stiffened compression flanges of box girders. *Thin-walled Struct.* **1**, 189–210.

Koiter, W. T. and Pignataro, M. (1974). An alternative approach to the interaction between local and overall buckling in stiffened panels. In *IUTAM Symposium, Cambridge/USA* (Edited by B. Budiansky), pp. 133–148. Springer, New York/Berlin/Wien.

Mansour, A. (1971). On the nonlinear theory of orthotropic plates. *J. Ship Res.* **12**, 266–277.

Marguerre, K. (1937). Die mittragende Breite der gedruckten Platte. *Luftfahrtforsch.* **14**, 121–128.

Neut, A. van der (1974). Mode interaction with stiffened panels. In *IUTAM Symposium Cambridge/USA* (Edited by B. Budiansky), pp. 117–132. Springer, New York/Berlin/Wien.

Smith, C. S. (1975). Compressive strength of welded steel ship grillages. *Trans. RINA* **117**, 325–359.

Timoshenko, S. P. and Gere, J. M. (1961). Theory of elastic stability. McGraw-Hill, New York.

Troitsky, M. S. (1976). *Stiffened Plates; Bending, Stability and Vibrations*. Elsevier Scientific, New York.

Tulk, J. D. and Walker, A. C. (1976). Model studies of the elastic buckling of a stiffened plate. *J. Strain Analysis* **11**, 137–143.

Tvergaard, V. (1973). Imperfection-sensitivity of a wide integrally stiffened panel under compression. *Int. J. Solids Structures* **9**, 177–192.

Tvergaard, V. and Needleman, A. (1980). On the localizations of buckling patterns. *J. Appl. Mech.* **47**, 177–192.

Ueda, Y. and Yao, T. (1983). Ultimate strength of compressed stiffened plates and minimum stiffness ratio of their stiffeners. *Engng Struct.* **5**, 97–107.

APPENDIX

Notation

- a length of stiffened panel
- b distance between stiffeners
- d total width of stiffened panel
- h height of stiffener
- b_f total width of flange
- t_f thickness of flange
- t_w thicknes of web
- A_s stiffener area, $A_s = ht_w + b_f t_f$, Fig. 2
- N number of stiffeners
- E Young's modulus of elasticity
- ν Poisson's ratio ($\nu = 0.3$ in examples)
- e_s eccentricity of stiffener forces, Fig. 7. $e_s = (\frac{1}{2}h^2 t_w + b_f t_f h)/A_s$ from moment equilibrium
- e_c^o eccentricity of neutral plane for combined stiffener plate section (Figs 4, 7)
  $e_c^o = N(\frac{1}{2}h^2 t_w + b_f t_f h)/(NA_s + dt)$

Relative area coefficients:

$$a_s = \frac{NA_s}{NA_s + dt} \qquad a_c = \frac{Nb_c t_c}{NA_s + dt}$$

$$a_s' = \frac{A_s}{A_s + bt} \qquad a_c' = \frac{b_c t_c}{A_s + bt}$$

$$a_s'' = a_s \frac{N+1}{N+a_s} \simeq a_s \quad \text{when } N \gg 1$$

$$a_c'' = a_c \frac{N+1}{N+a_s} \simeq a_c \quad \text{when } N \gg 1.$$

Coefficients:

$$f_1 = 2a_2$$
$$f_2 = a_1 + 6a_2\xi^2$$
$$f_3 = 2a_1\xi + 6a_2\xi^2$$
$$f_4 = \xi + \tfrac{1}{2}a_1\xi^2 + 2a_2\xi^3.$$

Coefficients:

$$\phi_1 = (\tfrac{1}{2}ht_a + b_f t_f)\,dt = \frac{1}{3}\frac{a_s + 2a_c}{N(1-a_s)}$$

$$\phi_2 = (\tfrac{1}{2}ht_a + b_f t_f)\,dt = \frac{1}{2}\frac{a_c + 2a_c}{N(1-a_s)}$$

$$\phi_3 = \operatorname{cotan}\frac{\pi}{2}\frac{1}{N+1}$$

$$\psi = \left(\frac{a}{d} + \frac{d}{a}\right)^2 + 12(1-\nu^2)(N+1)\left(\frac{d}{a}\right)^2\left(\frac{h}{t}\right)^2\phi_3.$$

Coefficients in the potential energy function V:

$$k_1 = -\frac{\pi^2}{8}\frac{N+a_s}{N}\left(\frac{t}{a}\right)^2$$

$$b_{11} = \frac{\pi^4 E(1-a_s)}{96(1-\nu^2)}\left[\left(\frac{t}{d}\right)^4\left(1+\left(\frac{d}{a}\right)^2\right)^2 + 12(1-\nu^2)(N+1)\left(\frac{t}{a}\right)^4\left(\frac{h}{t}\right)^2\phi_3\right]$$

$$b_{111} = -\frac{\pi^4}{3}Ev\left(\frac{t}{a}\right)^2\frac{h}{t}\left(\frac{t}{d}\right)^2(1-a_s)\phi_2\phi_3$$

$$b_{1111} = \frac{\pi^4}{256}E\left[(2a_s^2\nu^2 + 1 - a_s + a_s\nu^2)\left(\frac{t}{d}\right)^4 + \left(\frac{N-a_s}{N} - 2\left(\frac{a_s}{N}\right)^2\right)\left(\frac{t}{a}\right)^4\right].$$

Postbuckling coefficients:

$$a_1 = -\frac{48}{\pi}(1-\nu^2)\nu\frac{h}{t}\frac{\phi_2\phi_3}{\psi}$$

$$a_2 = \frac{3}{4}\frac{(1-\nu^2)}{1-a_s}\left(\frac{d}{a}\right)^2\frac{1}{\psi}\left[(2a_s^2\nu^2 + 1 - a_s + a_s\nu^2)\left(\frac{a}{d}\right)^4 + \frac{N-a_s}{N} - 2\left(\frac{a_s}{N}\right)^2\right]$$

$$c_2 = -\tfrac{1}{2}(1-\nu^2)\frac{N+a_s}{N^2\psi}\left(N\nu + \left(\frac{d}{a}\right)^2\right)$$

$$d_2 = \tfrac{1}{2}(1-\nu^2)\left[\left(1+\frac{a_s}{N}\right) + \nu a_s\left(\frac{a}{d}\right)^2\right]\left(\frac{d}{a}\right)^2\frac{N+a_s}{N(1-a_s)}\frac{1}{\psi}.$$